XVIII IMEKO WORLD CONGRESS
Metrology for a Sustainable Development
September, 17 – 22, 2006, Rio de Janeiro, Brazil

# MEASUREMENT OF PATTERNED WAFER SURFACE DEFECTS USING ANNULAR EVANESCENT LIGHT ILLUMINATION METHOD

*Toshie Yoshioka* [1], *Takashi Miyoshi* [1], *Yasuhiro Takaya* [1]

[1] Dept. of Mechanical Engineering and Systems, Osaka University, 2-1 Yamada-oka, Suita-shi, Osaka 565-0871, Japan,
e-mail: yoshioka@optim.mech.eng.osaka-u.ac.jp

**Abstract:** To detect particulate defects on patterned wafers of below 100nm design rule, we proposed a new detection method using evanescent light illumination. To verify the feasibility of the method, we performed fundamental experiments. The results show that particle with a size of 170nm on the patterned wafer surface with about 400nm pitch is detected.

**Keywords:** near field optics, wafer inspection, nano-mesurements

## 1. INTRODUCTION

To realize high productivity and reliability of the semiconductor, patterned wafers inspection technology to maintain high yield becomes essential in modern semiconductor manufacturing processes [1]-[2]. To meet the demand for higher performance on integrated circuits (ICs), the semiconductor manufacturing processes focus attention on smaller circuit features and higher circuit density. As circuit feature is scaled below 100nm, the conventional defects inspection technology based on the imaging optics ultimately reaches the diffraction limit imposed by the wavelength of incident laser beam. The conventional technology based on the light scattering systems using the propagating light illumination cannot distinguish the particle signal from the background light scattered by the patterned wafer of less than 100nm design rule. So, we propose a new defect detection method based on near field optics for evaluating the typical particulate nano-defects ; for example dusts and contaminations on a patterned wafer surface. Instead of the propagating laser beam like conventional method, our proposed method uses the evanescent light that doesn't propagate but is localized, so that the background light scattered by a patterned wafer surface is negligible. Therefore by using the proposed method based on evanescent light illumination, it is expected to sensitively detect the defects with the size of nanometer scale.

## 2. DEFECT DETECTION METHOD

Optical arrangement in two mediums is shown in fig.1. Two mediums border at z=0. Incident medium (Medium1) has a lower refractive index than Mesium2. A beam of light is incident on the border surface at an incident angle $\theta_1$. In the case of total internal reflection when $\theta_1$ is equal to or greater than the critical angle $\theta_c$, evanescent light $E$ is obtained by solving Maxwell equations under the boundary condition as follows,

$$E = A\exp\left(-k_2 z\sqrt{\left(\frac{n_1}{n_2}\right)^2 \sin^2\theta_1 - 1}\right)\exp\left(ik_1 x\sin\theta_1\right)\exp\left(i\omega t\right) \quad (1)$$

where, A is amplitude of incident light, $k_1$ and $k_2$ are wave number in the medium1 and in the medium2 respectively, $\omega$ is angular temporal frequency. First term of formula (1) shows that amplitude of evanescent light decays rapidly in the z-direction proportional to exp(-z), becoming faint at a distance of only a few wavelength. Second term shows that evanescent light advances in just the x-direction. We proposed a new particle detection method using the characteristics of evanescent light.

Fig.2 presents the concept of our proposed method. A converging annular light used as light source is incident on the micro-hemispherical lens [3]. When the converging angle is larger than the critical angle, the total internal reflection condition is met at the bottom of a hemispherical lens. So, annular evanescent light is generated at the bottom.

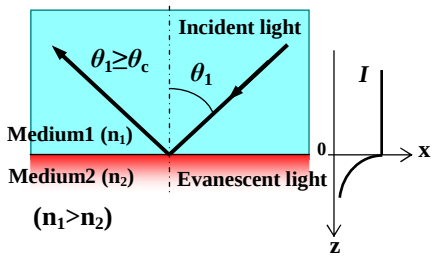


Fig.1 Generation of evanescent light

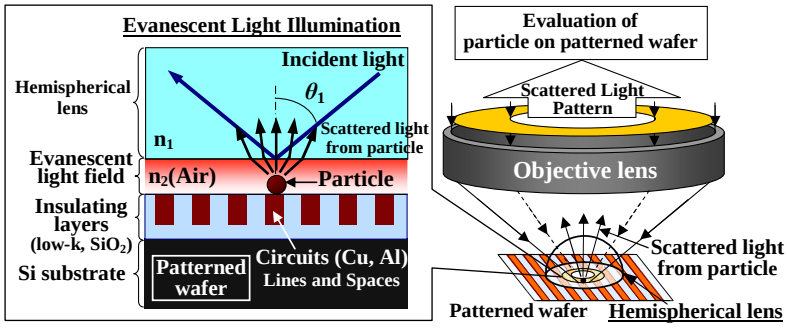


Fig. 2 Concept of particle detection using annular evanescent light illumination

The annular evanescent light illuminates the patterned wafer surface with a clearance of several hundred nanometers. Evanescent light is localized near by the bottom surface and decays exponentially away from the bottom surface. So the evanescent light effectively illuminates just the particulate defects on the patterned wafer surface, because it fades out at the patterned wafer surface. The proposed method can evaluate the particulate defect on a patterned wafer surface by detecting the scattered light pattern from the particulate defect. The types of the particulate defects can be identified based on scattered light pattern variation.

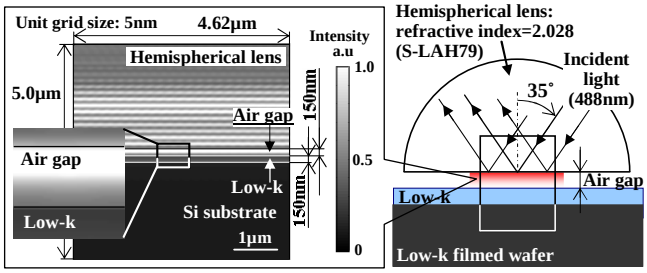


**Fig.3 Simulation model and result**

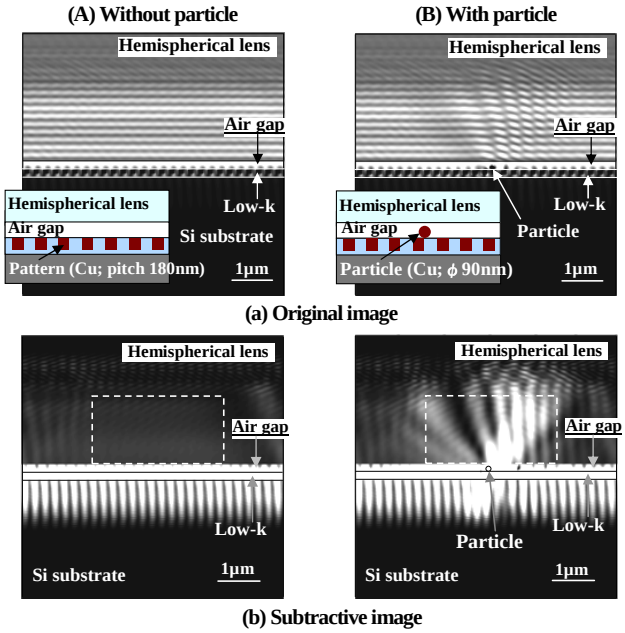


**Fig.4 Simulation results of patterned wafer model**

## 3. NUMERICAL ANALYSIS

In order to analyze evanescent light scattering problem numerically, we have developed a computer simulation to solve Maxwell's equations based on the 2-dimensional Finite-Difference Time-Domain (FDTD) method [4]. First, we set a simple model as depicted in fig.3. The grid size and the volume are given by 5nm and 924×1000 grids. $Ar^+$ laser (wavelength=488nm) source is placed in topside X-plane and the incident angle is taken at 35˚. The refractive index of hemispherical lens $n_1$ is 2.028. Considering the critical angle $\theta_c$ of 29.54˚, the incident light is totally reflected at the boundary surface, that is the bottom of the hemispherical lens. The simulation result shows evanescent light is generated under the bottom of the hemispherical lens. Next, we set a patterned wafer model shown in fig.4. Low-k film of 150nm in thickness on Si wafer and the hemispherical lens as mentioned above are set with air gap of 150nm. Linear Cu circuit pattern with the pitch of 180nm with a depth of 90nm is included in low-k film layer. A Cu particle with the size of 90nm in diameter is placed on the patterned wafer surface. The simulation results are shown in fig.4(a). With the particle in fig.4(a)(B), the particle scatters the evanescent light and scattered light pass through the hemispherical lens. To evaluate the scattered light in more detail, the simulation results of patterned wafer model are subtracted from the results shown in fig.3. By comparison between (b)(A) without particle and (b)(B) with particle, the scattered light intensity from the particle is clearly higher than by the patterned wafer surface. Additionally to evaluate quantitatively, we compute amount of light intensity inside the dotted area in the each subtractive image. The scattered light intensity is 4119 in (B), and is 1038 in (A). Therefore the scattered light intensity from a particle on the pattern wafer surface has a high value to be about 4 times of one by the pattern wafer surface without a particle.

## 4. EXPERIMENTAL SYSTEM

Fig.5 presents the schematic diagram of experimental system. As a light source, the $Ar^+$ laser with the wavelength of 488nm is used. An annular beam transparency filter with a light blocking film in the central part transforms the incident Gaussian beam into a annular beam. The annular beam converges at the bottom of a hemispherical lens (material: S-LAH79 (refractive index=2.028)) through an objective lens with focal length $f_0$=2mm. As sown in fig.5(A), the tapered hemispherical lens is used to avoid the collision between the bottom surface of the hemispherical lens and the sample surface caused by relative tilt. It is designed to meet the condition that the bottom size is larger than the converging annular beam size, that is the bottom size of about 100µm in diameter. The tapered hemispherical lens is bonded with the alumina $Al_2O_3$ plate whose thickness is 100µm, so that the bottom of the tapered hemispherical lens is protruded from the plane with the gap of 100µm. The objective lens and the tapered hemispherical lens are positioned precisely by the piezo electric translator in the vertical direction. The hemispherical lens is moved in the horizontal direction using a micrometer caliper, and the optical axis of the hemispherical lens is adjusted to the optical axis of the objective lens. The scattered evanescent light from the sample is gathered by the objective lens, and detected using a sensitive CCD area sensor whose pixel size is 6.7 µm square. The sample is set at the XY-fine positioning unit with stepping motor.

The illumination characteristic of the optical system is verified. Fig.6(a) illustrates the schematic diagram of an optical Fourier transform system. At smaller angle than the critical angle $\theta_c$ of 29.54 degree, the light incident to the bottom of the hemispherical lens is transmitted. When the incident angle is equal to and larger than the critical angle $\theta_c$, the incident light is totally reflected at the bottom of the hemispherical lens and the evanescent light is generated under the bottom. The boundary between the transmitted light and the reflected light corresponds to the critical angle.

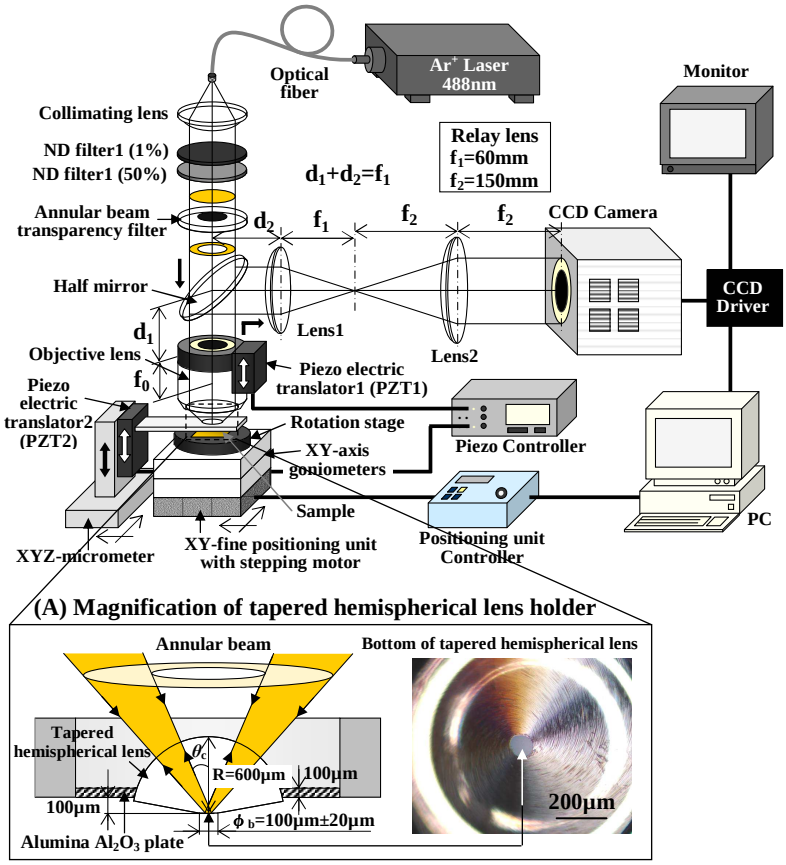


Fig.5 Schematic diagram of experimental system

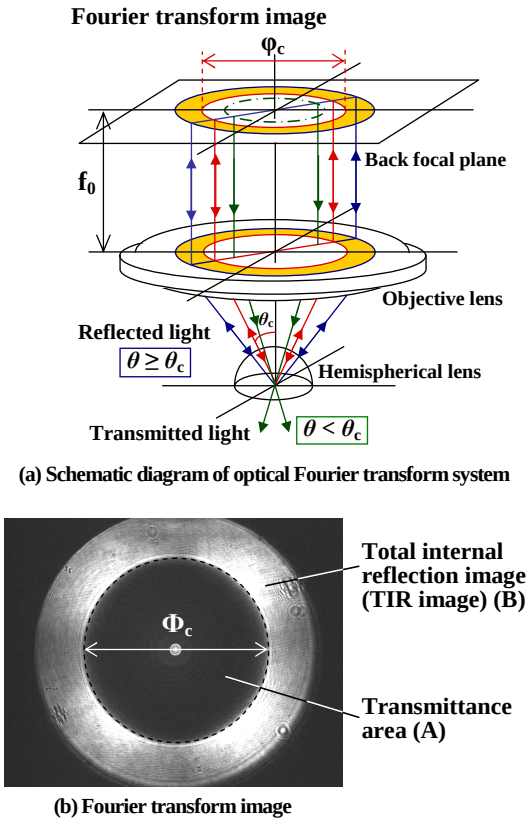


Fig.6 Fourier transform image using annular evanescent light illumination

The diameter of the transmitted light $\varphi_c$ is about 4.93mm as calculated under the optical condition. Fig.6(b) shows Fourier transform image without the annular beam transparency filter when the focal point of the objective lens is adjusted to the bottom of the hemispherical lens. As shown in fig.6(b), the transmittance area (A) and the total internal reflection image (TIR image) (B) are seen. The boundary between the transmittance area and the TIR image corresponds to the critical angle. The diameter of the TIR image $\Phi_c$ is about 4.91mm (=733pixel multiplied by 6.7μm/pixel). So, the actual dimension $\Phi_c$ is nearly equal to the calculated one $\varphi_c$. Therefore, TIR image (B) is the evanescent light illumination area and we focus attention on TIR image (B).

## 5. EXPERIMENTAL RESULTS

To verify the feasibility of our proposed method, we carried out the basic experiments.

### *4.1 Detection of scattered light pattern*

As a scattering object using the tip of the silicon AFM probe with a size of about 130nm, the detection experiments of the scattered light pattern from the tip is performed. Fig.7 shows the SIM (Scanning Ion Microscope) image of the AFM probe. This probe is set at the XY-fine positioning unit with stepping motor.

Fig.8 presents the setup arrangement for experiments. The tip of the AFM probe contacts the bottom of the hemispherical lens. The focal point of the objective lens is set at 13μm above the bottom. In the Fourier transform image, the probe is placed on the lower side of the TIR image. From this arrangement, the hemispherical lens is being moved 250nm upward. Fig.9 shows the detection of scattered light pattern from the tip of AFM probe. As shown in fig.9(a), the scattered light pattern form the tip is seen on the lower side of TIR image when the tip contacts the bottom. In fig.9(b) when the distance between the tip and

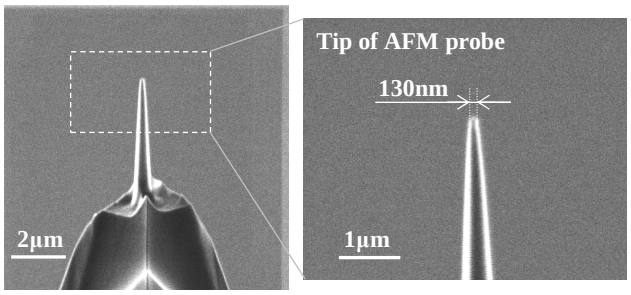


Fig.7 SIM image of AFM probe

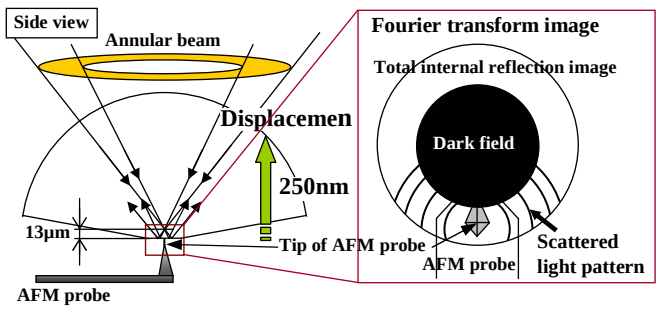


Fig.8 Setup experiments (Tip of AFM probe)

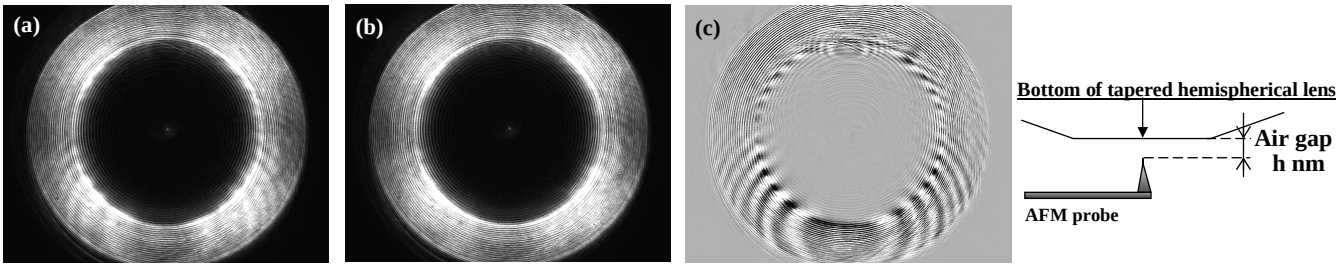


**Fig.9 Detection of scattered light pattern from tip of AFM probe**
**(a)Estimated contact position (b)air gap =250nm (c)=(a)-(c) subtractive image**

the bottom of the hemispherical lens (air gap) is 250nm, the scattered light is not observed. This is because the tip is out of evanescent light localized at the bottom. Fig.9(c) is the enhanced scattered light obtained by subtracting (a) from (b). The scattered light is clearly observed. The proposed system detects the scattered light pattern from the tip, which is considered to be reflected the shape of the tip. These results suggested that the proposed method enables detect the nano-defect.

### *4.2 Investigation of background noise*

To investigate the influence of background scattering caused by a patterned wafer surface, the fundamental experiments are conducted using a line sample as simplest pattered wafer sample shown in fig.10 (210nm in width, 11µm in length, 520nm in height). This was fabricated on a silicon wafer surface using CVD (Chemical Vapor Deposition) operation of FIB (Focused Ion Beam) process.

Fig.11 presents the initial arrangement. The line sample is adjusted in the center of the Fourier transform image. The hemispherical lens is moved up to 250nm from the initial position that the bottom surface of the hemispherical lens contacts with the top of the linear deposition. Fig.12 shows the background scattering images changing with the distance between the bottom of hemispherical lens and the top of the linear depositiom (air gap). In fig.12(a), when the tip contacts the top, the background scattering image which is considered to reflect the shaps of the line sample is obseved. The background scattering image fades out as air gap is wider. Fig.13 shows the relation between air gap and intensity measured amount of light intensity inside the area C. The intensity decreases rapidly according to widening air gap. This reflects the characteristics of the evanescent light of which intensity decays rapidly as shown in formula(1). When air gap is wider than 170nm, the intensity is lower. In fig.12(c) at the air gap of 200nm, the background scattering image fades out. So, Fig.12 and Fig.13 indicate that the background scattering by the line sample is negligible when air gap is wider than 170nm.

### *4.3 Measurement of particulate defect on patterned wafer sample*

The patterned wafer surface with particulate defect of 170nm is measured. Fig.14 shows the manufacturing process of the sample. First, 200nm polystyrene latex spheres are scattered on Silicon AFM cantilever surface. Next, the surface is coated by gold evaporation. Thirdly, using ion beam etching operation of FIB, the linear circuit pattern is fabricated. Fig.15 shows the AFM image and the cross section of the particulate defect on the pattered wafer

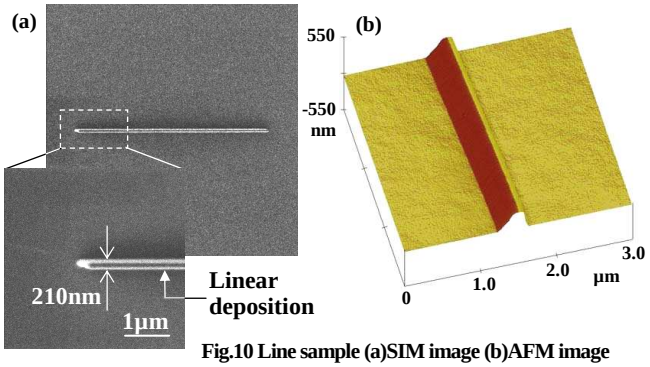


**Fig.10 Line sample (a)SIM image (b)AFM image**

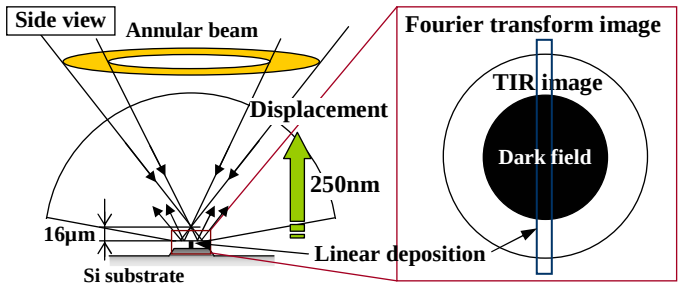


**Fig.11 Setup experiments (Line sample)**

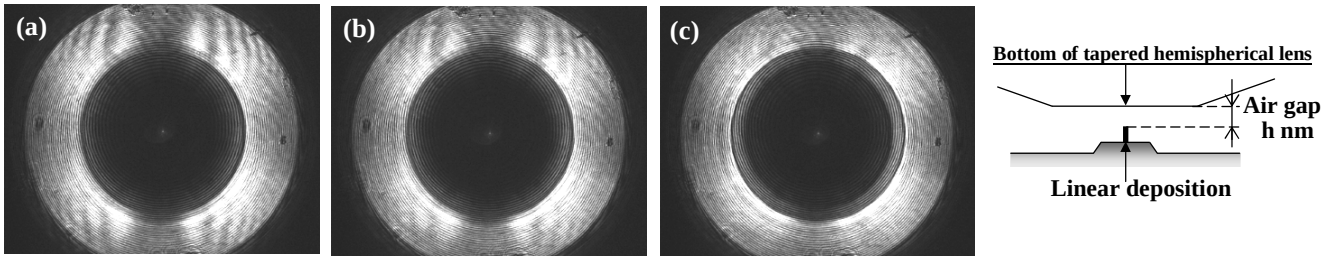


**Fig.12 Background scattering images changing with air gap**
**(a)Estimated contact position, Air gap is (b)50nm (c)200nm**

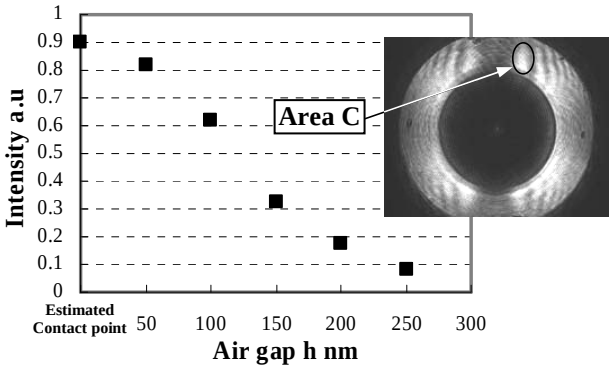


**Fig.13 Relation between intensity of area C and air gap**

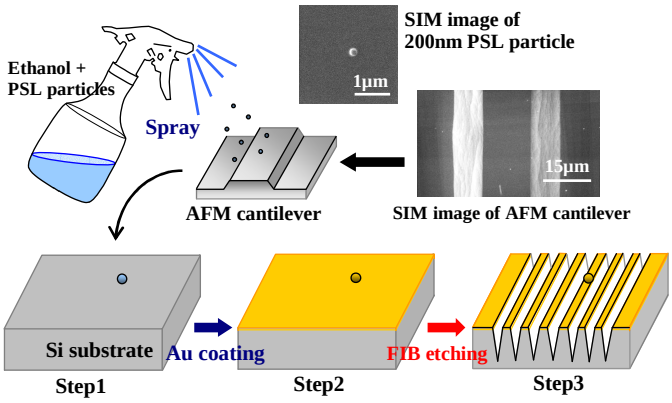


**Fig.14 Manufacturing steps of particulate defect on patterned wafer sample**

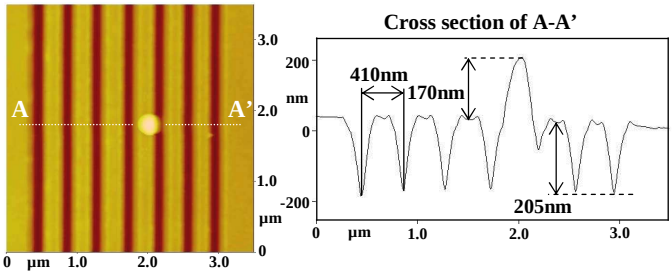


**Fig.15 AFM image and the cross section of particulate defect on patterned wafer sample**

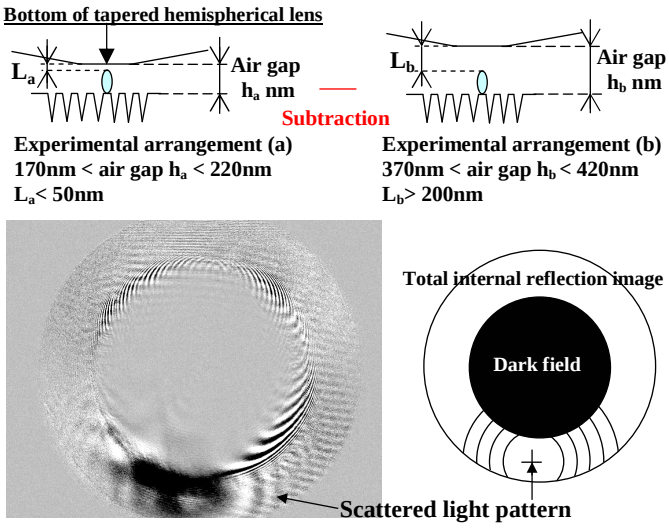


**Fig.16 Subtractive image of scattered light pattern caused by particulate defect on patterned wafer sample**

sample of about 200nm pitch (205nm in depth).

As shown in fig.16, air gap indicates the distance between the bottom of hemispherical lens and the patterned wafer surface. In the experimental arrangement (a) when air gap is wider than 170nm and narrower than 220nm, the clearance between the bottom and the top of particulate defect ($L_a$) is under 50nm. By setting the air gap to be wider than 170nm, background scattering image by patterned wafer surface isn't detected at all. The evanescent light illuminates just the particulate defect. In the experimental arrangement (b) at 370nm< air gap < 420nm, the clearance $L_b$ is wider than 200nm. The particulate defect is out of evanescent light localized at the bottom. By subtracting operation of both the Fourier transform images, the scattered light pattern as shown in fig.16 is obtained on the lower side of TIR image, which is considered to reflect the shape of the particulate defect. These results suggest that the particulate defect can be detected without the influence of the background scattering by patterned surface.

## 5. CONCLUSION

A new defect detection method for evaluating the nano-defect on the patterned wafer surface by evanescent light illumination is proposed. The fundamental characteristics of this proposed method using FDTD simulation is analyzed. The simulation results show that the proposed method is effective for detecting 90nm size particle on the patterned wafer of 180nm pitch with S/N ration of about 4.0. The basic experiments show that the background light scattered by a patterned surface is negligible when the air gap is wider than 170nm. In this condition, the defect with a size of 170nm on the patterned wafer surface of about 400nm pitch is successfully detected.

## REFERENCES


[1] KLA-Tencor, Yield Management SOLUTIONS, VOLUME5, ISSUE1, SPRING 2003

[2] Nikkei Business Publications, NIKKEI MICRODEVICE, 6, 228 (2004) 28-49.

[3] S.M.Mansfield and G.S.Kino, "Solid immersion microscope", Appl.Phys.Lett, 57 (1990) 2615

[4] T.Ueno, "Finite Difference Time Domain Method for Electromagnetic Field and Antennas", CORONA PUBLISHING, Japan, 1998